AJCPP 2008
March 6-8, 2008, Gyeongju, Korea

Investigation on the Off Design Performance of a Transonic Compressor with Circumferential Grooves

ZHU Jianhong, PIAO Ying, Zhou Jianxing, Qi Xingming
School of Aerospace, Tsinghua University, China
Building 28# Room 436, Tsinghua University, Beijing, China 100084
Zhujh04@mails.tsinghua.edu.cn

Keywords: Aerospace Propulsion System, Compressor, Casing Treatment, Numerical Simulation, Stall

Abstract

Two cases with circumferential grooves were designed for a transonic compressor, and 3-D numerical simulations were conducted for stall mechanism at three representative speeds. A conclusion can be drawn from the comparison between compressors with or without casing treatment that: with the rising of rotation speed, stall margin increases dramatically under the help of casing treatments, and the case with middle grooves has reasonable compromise between stall margin increment and efficiency cutting. At lower speed, the increment reduces, and grooves at the back of blade tip have more influence on stall margin. Further investigation shows there is a transition in mechanism of compressor stall with the decline of rotational speed: at high rotation speed, the expansion of stall margin mainly results from the suppression of tip leakage vortex by casing treatments, yet it benefits more from the depression of boundary layer separation from suction surface of blade tip.

Introduction

Since Hartman accidentally found out in an experiment that honeycomb case could improve the stall margin of compressor while no gas was discharged, extensive application researches have been performed in many countries. It has been widely applied in various kinds of axial flow compressors, such as CF-56, АЛ-31Ф, РН-33/РН-93,F100 et. However, most of the designs were based on experiments from. In fact, the actual application is ahead of theory research, and design mainly depends on the experience of engineers.

With the development of computational fluid dynamics (CFD), it is possible to simulate the steady or unsteady flow in the casing treatment. Due to various reasons, most of these work focus on the expansion mechanics of stall margin under design condition, while off-designed mode is seldom concerned. As a matter of fact, stall margin problem for a special engine always takes place in the process of start, stop and transition. Therefore, the performance of casing treatment at three typical rotation speeds of 100%N, 80%N and 60%N was researched on NASA rotor37 in order to find some basic principles for casing treatment design. In this paper, circumferential grooves were adopted because of its simple structure.

Compressor and casing treatment structure

Rotor 37 was designed and initially tested as part of a research program involving four related axial-flow compressor stages by NASA Glenn Research Center in 1970s. In the case of rotor 37, representative values are listed in Table 1, more detailed parameters and performance experiment results can be found in reference [2, 3]. In 1993, it was adopted by ASME as a blind test case of CFD code to evaluate the quality of numerical computer simulation for turbo machine performance and flow field details. The experiment data and test results were published in the following year's ASME conference. Hence it has been selected as one of the standard testing cases for CFD code evaluation on turbo machine [4].

Table1. NASA rotor37 parameters

parameter	value
Choke Flow/(kg/s)	20.93
Pressure ratio	2.106
Rotational speed/(rpm)	17188.7
Tip gap/(mm)	0.356
Inlet hub-to-tip diameter ratio	0.7
Tip solidity	1.29
Tip tangential speed/(m/s)	454.14

A casing treatment with five grooves, which are averagely distributed from leading edge to trailing edge on the chord of blade tip, was designed based on the data from reference [5]. The tooth width is almost equivalent to the maximum thickness of blade tip 1.8mm, and groove breadth is double that of the tooth. Many researches have reported no more impact has been found on the stall margin after groove depth exceeds certain level. Thus groove depth is selected as 12mm, which is almost triple of the groove width. Those treatment grooves rang from 0.7% chord at the front of blade tip to the back of 92%, see fig1. Grooves' number is 1 to 5 from the inlet. No.1 groove is removed because it's negative effect on stall margin in lots of simulations.

Description of CFD-model for simulation

The commercial solver Fine/Turbo was used in present study. And 3D Reynolds-averaged Navier-Stokes equations were discretized in space using a cell-centered finite volume formulation and in time using an explicit four-stage Runge-Kutta method. The one equation turbulence model of Spalart-Allmaras was employed to estimate the vortex viscosity. All equations were solved with local time stepping, implicit residual smoothing, and multi-grid techniques for the sake of computation time.

Fig.1 shows a composite grid system with structured grids. In main flow region, a block structured topology with H-blocks for the inlet and outlet. An O-block for rotor blade was applied to model rotor blade passage. Blade tip was divided into two layers. Bottom layer used H-block surrounded by butterfly mesh, while the upper one applied H-block, whose bottom surface was connected to main flow by full non matching connection (FNMC). Grooves of H-block were also connected to the top of upper layer by FNMC. Due to the axisymmetric structure of grooves and rotor, it's enough to steadily research a single blade passage. Various combination of grooves represent different casing treatment. In this paper, smooth case, four grooves at the back of blade tip(case-back4) and two grooves in the middle of blade tip (case-mid23) were studied, and experiment data under smooth case was presented as reference.

The whole mesh of main blade passage consists of 41 cells in pitchwise(I) direction, 65 cells in spanwise (J) direction, and O-grid has 241 cells around rotor blade in the circumferential direction to ensure a high quality mesh at the leading and trailing edge. Tip clearance was modeled by 17 grid points in radial direction. In order to build a common layer for grooves, the blade tip mesh and main grid were divided into two layers, the upper layers were completely replaced from inlet to outlet. It is necessary to point out that the split point of tip mesh block in spanwise must be carefully chosen; otherwise multi-grid technique is not available.

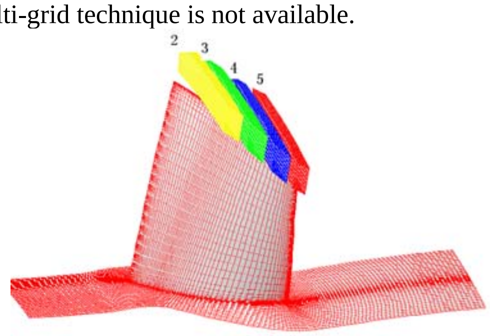

Fig.1 Grids of rotor37 with casing treatment

Boundary conditions: to simulate the flow field at the same condition of experiment, the inlet and outlet boundary conditions were given at the measurement positions of experiment. Average distributed total pressure and total temperature were applied in axial direction at inlet. And back pressure was specified on the hub at outlet, while radial equilibrium equation was employed to calculate hub-to-shroud profile of static pressure. On the hub and blade wall, corrected rotation speed of 17188.7rpm and insulation condition was set. Period conditions were applied on the left and right surfaces of main blade passage and grooves.

Results and analysis

The calculation began from choke point of compressor, and static pressure increment steps of 0.5bar to 200pa at outlet were applied to accurately locate the boundary of stall. Detailed calculations were conducted near the highest efficiency point to locate peak value more exactly. The mark of numerical stall appears as a transient flow field characterized by continuous decrease in mass flow, total pressure ratio and efficiency [7,8]. However, it is never a purely numerical phenomenon, but always arises from physical consequences due to distinctive flow mechanisms.

Rotor performance

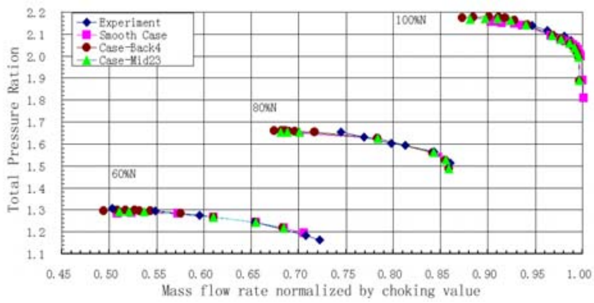

a) Total Pressure Ratio

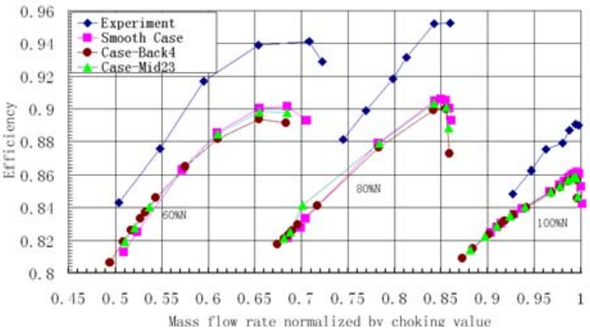

b) Adiabatic Efficiency

Fig.2 Rotor 37 rotor performance

Total pressure ratio and adiabatic efficiency under all cases and experiment data of smooth case are expressed in fig.2. The curves of total pressure ratio are in a satisfying agreement with the experiment, while adiabatic efficiency curves have a maximal error of 4%. That efficiency problem seems to be common for the diversified results from different researchers, so does the ASME test.

Adiabatic efficiency always descends after casing treatment. The lower rotation speed, the worse efficiency loss is observed. Due to the release effect of casing treatment, mass flow became higher than untreated case at the same back pressure. In other words, operation point of the whole engine may be readjusted. According to the definition of stall margin, it is related with the minimum mass flow and the pressure ratio at that point. The latter one had no so obvious variation as minimum mass flow after casing treatment. Therefore the stall boundary was primarily expanded by the decline of mass flow.

Stall margin expansion at high speed

As indicated by experiment data and CFD simulations of several authors, the tip leakage vortex in the rotor blade passage undergoes a dramatic change in topology if rotor is operated near surge in highly loaded transonic compressor stage. Tip leakage vortex tends to break down due to the high friction losses inside the vortex core when pressure ratio exceeds certain limitation [9,10,11].

Figure 3 shows tip streamlines of untreated and mid23 case at design speed while mass flow is about 90% of the choking value. Under smooth case (fig.3.a), blade tip leakage vortex originates from the interaction of main stream flow and leakage airflow, The latter one flows over the blade tip from pressure surface to suction surface. With the rising of back pressure, the center of leak vortex moves towards pressure surface on adjacent blade. Part of leakage fluid is sucked in by interstitial fluid in adjacent tip gap. Vortex intensity starts to weaken until it disappears completely at about 30% tip chord near next pressure surface. Meanwhile, low velocity zone expands quickly in circumferential and radial directions. In the end, blade passage is blocked and compressor stalls.

When case was treated with middle 2nd and 3rd grooves, tip leakage vortex is sucked into grooves in high pressure zone and circumferentially transported over blade tip to reinject the main flow in low pressure zone (fig.3.b). The tip leakage vortex is not completely destroyed by mid23 grooves, but its intensity is significantly reduced in contrast with that of untreated case. Thus mainstream fluid can flow out more easily, and flow speed increases. The jam caused by leakage vortex is relieved and compressor stall is postponed.

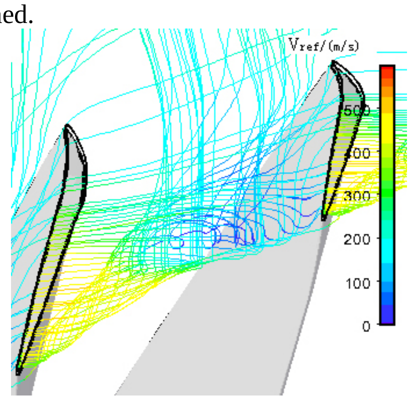

a) Smooth case under 90.34% mass flow

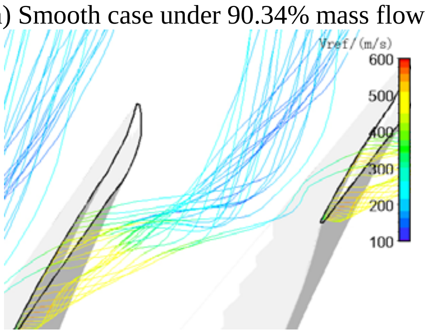

b) Case-mid23 under 89.8% mass flow

Fig.3 Tip streamlines of smooth and mid23 case around 90% mass flow at 100%N

See fig.4 for relative Mach number of aforementioned cases and operation mode at 99% span. The low velocity area of mid23 is smaller than that of smooth case, and speed of core flow rises from 0.055Ma to 0.45Ma. In addition, even on the condition of near surge, the pitch-wise scale of separation region on suction surface is far smaller than that of the breakdown zone by leakage vortex (fig.4.a). Current stall hereby is not caused by separation of blade profile, but the abruption of leakage vortex, which builds up a low-energy flow zone, and forces compressor to operate towards stall by blocking the passage at blade tip.

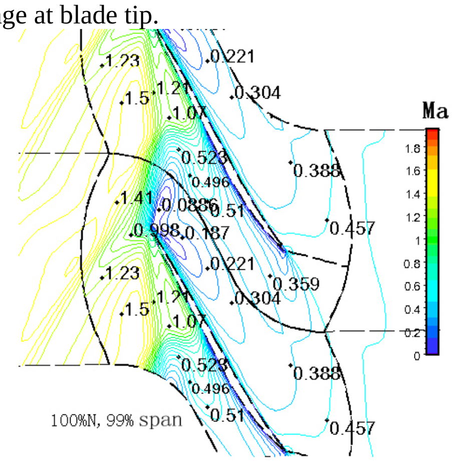

a) Smooth case under 90.34% mass flow

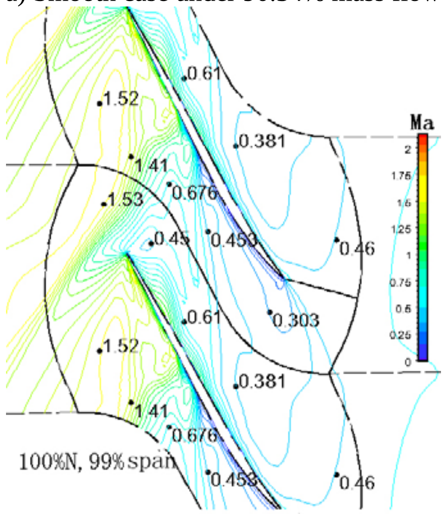

b) Case-mid23 under 89.8% mass flow

Fig.4 Relative Mach number of smooth and mid23 case around 90% mass flow

Fig.5 shows the relative total pressure loss coefficient (Cp) of smooth and mid23 case at the section of 79.5% chord. The blockage primarily occurs at the mid part of blade tip passage in pitch-wise direction. Casing treatment degrades Cp and releases the airflow jam in passage (fig.5.b). However, the loss increases near left suction surface after casing treatment, so does the scope. It can be explained by the mixing and diffusion when air reenters main stream from radial direction after being circumferentially transported in grooves. This process redistributes the jam zone and degrades compressor efficiency.

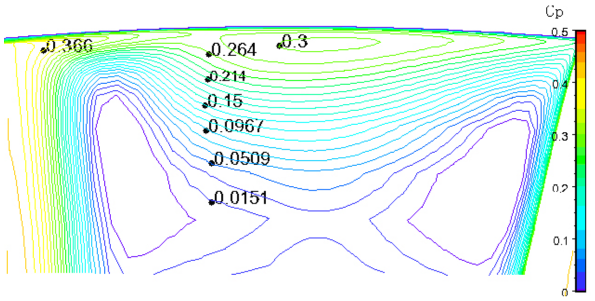

a) Smooth case under 90.34% mass flow

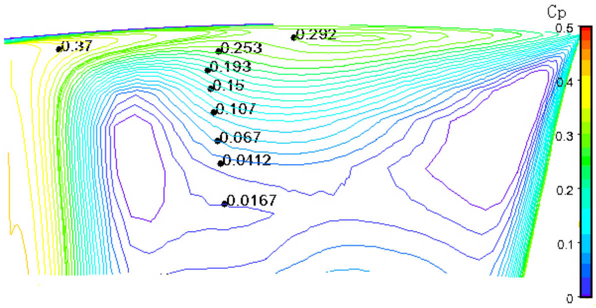

b) Case-mid23 under 89.8% mass flow
Fig.5 Cp of smooth and mid23 case at 100%N and section of 79.5% chord

Stall margin expansion at low speed

Mass flow of compressor decreases at low er rotational speed. Attack angle of blade profile increases due to lower axial velocity, and airflow tends to separate from blade back. In addition, leakage flow from pressure surface to suction one aggravates that separation near blade tip. As a result, jam mainly occurs at the back of blade tip. That's obviously different from the state at higher rotation speed. See fig.6 for relative Mach number of smooth and back4 case at 60%N and 99% span. Low speed zone caused by air separation from suction surface almost covers 2/3 of blade passage. In fig.6.b, that separation at the back of blade tip is suppressed remarkably after casing treatment.

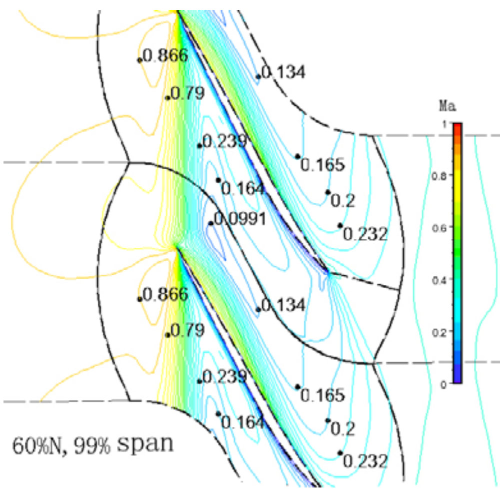

a) Smooth case under 50.9% mass flow

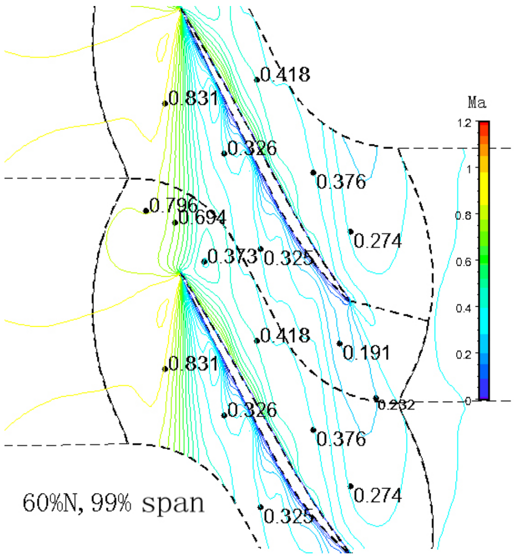

b) Case-back4 under 50.9% mass flow
Fig.6 Relative Mach number of smooth and back4 case at 99% span around 50% mass flow

Fig.7 shows Cp of smooth and back4 casing treatments at the section of 79.5% blade chord and 60%N. Main loss in spanwise focuses on the suction surface of blade tip due to the increase of inlet attack angle and leakage flow, and compressor primarily stalls from the blade tip. The scope of high loss zone along spanwise decreases, and central total pressure loss comes down from 0.243 to 0.229 after casing treatment. In brief, circumferential grooves improve flow condition at blade tip through sucking the low-energy air in flow separation zone near suction surface, and broaden the stability boundary of compressor.

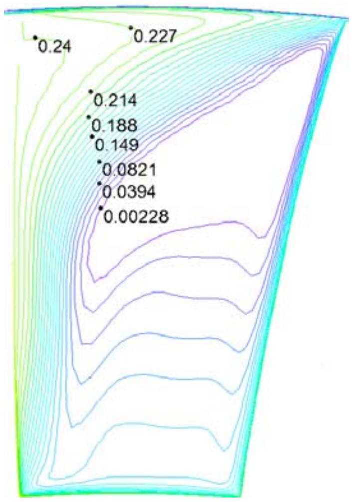

a) Smooth case under 50.9% mass flow

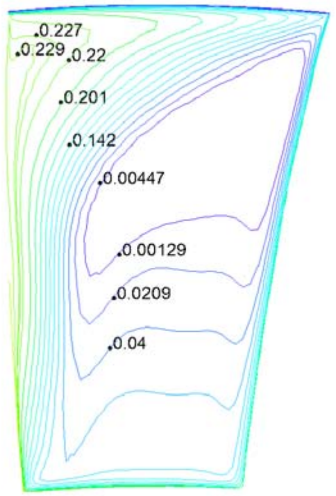

b) Case-back4 under 50.9% mass flow
Fig.7 Cp of smooth and back4 case at section of 79.5% chord and 60%N

Position of grooves

In this study, five grooves were design for rotor37. However, the first groove in the front of blade tip was found to be negative to the stability of compressor during simulation. Intense mixing occurs when air in 1st groove jets into main flow, and passage shock is pushed upward. Blade passage is blocked seriously at the fore part of blade chord. Therefore 1st groove is not discussed here any more. See fig.2 for calculated and experimental performance of case-mid23, case-back4 and smooth case. Table2 shows simulation results under various cases. The stall margin is defined at equal corrected rotational speed by equation 1. The reference point of stall margin is not selected as the intersection point of work line and corrected rotational speed as usual. In this paper, only relative stall margins under various casing treatments are concerned, numerical calculation points of highest efficiency under smooth case at various rotation speeds are selected as reference.

$$SW=\left[\left(\left(\frac{\pi_c}{W_{a,c}}\right)_1-\left(\frac{\pi_c}{W_{a,c}}\right)_0\right)\Big/\left(\frac{\pi_c}{W_{a,c}}\right)_0\right]\times 100\% \qquad (1)$$

SW : stall margin, π_c : pressure ratio,

$W_{a,c}$: corrected mass flow.

Table2. Calculated stall margin under various cases

Cases	Rotatioal speed	Mass flow of reference point	Efficiency of reference point	Pressure ratio of reference point	Stall margin/%	Stall margin increment
Smooth	100%N	0.996	0.8613	2.02	17.73	0.00
Mid23	100%N	0.996	0.8529	1.95	25.88	8.15
Back4	100%N	0.996	0.8505	1.93	28.42	10.69
Smooth	80%N	0.850	0.9058	1.55	31.70	0.00
Mid23	80%N	0.850	0.9021	1.54	33.70	2.00
Back4	80%N	0.850	0.8998	1.54	35.95	4.25
Smooth	60%N	0.685	0.9013	1.22	41.93	0.00
Mid23	60%N	0.685	0.8977	1.22	42.33	0.40
Back4	60%N	0.685	0.8911	1.22	47.60	5.67

In fig.2, simulations of smooth case at different rotation speeds acquire lower stall mass flow than experiment. On one hand, it can be attributed to the turbulence model's incapability for accurate stall prediction. On the other hand, all of the simulations were conducted under perfect conditions, yet experiment had so much uncertain factors, such as dynamic rotational speed, mismachining tolerance, measure inaccuracy and inlet distortion etc. Although the absolute value of stall mass flow is somewhat over predicted, the errors should be consistent for different casing treatments. The relative values are reliable on condition that same turbulence model, similar grid, and identical boundary condition are applied.

As efficiency is concerned, it is inverse proportional to the number of grooves. The less grooves, the higher efficiency is observed because the process produces entropy increment when compressed air is released into groove, and reenters main stream after being circumferentially transported.

According to the stall margin increments in table 2, a general trend is drawn that effect of casing treatment enhances with the rising of rotational speed whatsoever mid23 or back4 case. It's obvious that grooves of mid23 have neglectable effect (0.4% stall margin increment) on compressor stability at lower speed. As the rotational speed declines, the primary factor of compressor instability is not the leakage vortex breakdown at blade tip any more, but the boundary layer separation from suction surface because of over attack angle. To the latter case, separation zone at the back of blade tip enlarges with axial chord. Compare the relative Mach distribution of mid23 at 99% span in fig.8 with that in fig.6.a, the two grooves in the middle part of blade chord improve flow condition at the front part of blade tip by sucking separated gas. However, that separated zone grows rapidly while no groove is set at the back. Such phenomenon is no observed at back4 case in fig.6.b. In other words, the back grooves play more significant role in the expansion of stability boundary at lower speed.

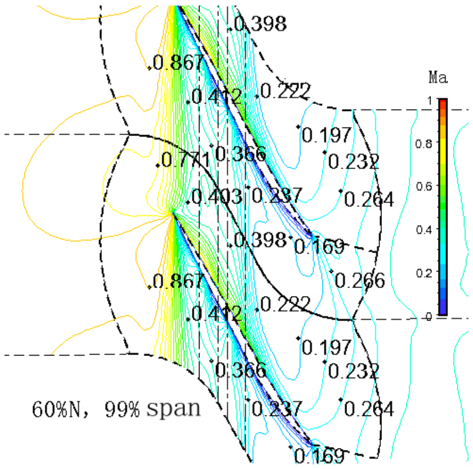

Fig.8 Relative Mach number under 51% mass flow of mid23 casing treatments

Conclusion

1) The stall of transonic compressor stall near design rotational speed is mainly due to the jam caused by the leakage vortex breakdown at blade tip. That jam zone mainly focuses at the middle part of

blade tip; therefore circumferential grooves should cover the mid-chord to wipe off low-energy flow in that region.

2) At lower rotational speed, the mass flow of compressor is small, and boundary layer separates from blade suction surface under the cooperation of blade tip leakage flow and over-attack angle, which eventually leads to compressor stall. Thus more focus should be laid at the back of blade tip in casing treatment.
3) Amount of grooves is inverse proportion to the compressor efficiency. In actual practice, the operation rotational speed and stage number of casing treatment should be determined firstly in multi-stage compressor design, and the groove should be decreased as less as possible. If stall boundary expansion during start process is concerned, grooves should be laid at the back of blade tip to counteract the effect from over-attack angle.

References

1) Lu xingen, Chu wuli. Research and comment on the casing treatment of axial compressor[J]. Advances in Mechanics. 2006, 36（2）：222-223
2) Dunham J. CFD validation for propulsion system component, AGARD AR-355,1998
3) Suder L L. Experimental and computational investigation of the tip clearance flow in a transonic axial compressor rotor, NASA TM 106711,1989
4) Li Minjiang. Numerical Investigation and Design of Transonic Compressors with Tip Clearance Flow Using Multi-block Mesh. [Ph.D. Degree].Beijing: Beijing University of Aeronautics and Astronautics. 2004
5) Baily E E. Effects of grooved casing treatment on the flow range capability of a single stage axial-flow compressor. NASA TM X-2459,1972
6) Wang yongming, Hu jun, Tu Baofeng etc. Unsteady Numerical Simulation of Transonic Fan with Casing Treatment [J]. Journal of Nanjing University of Aeronautics & Astronautics, 2006, 38(5): 540-544
7) Lu Xinggen, Chu Wuli, Zhang Yanfeng. Numerical investigation of interaction between casing treatment and tip leakage flow in a transonic compressor rotor [J]. Journal of Xi’an Jiao Tong University. 2006, 40(11): 1357-1360
8) Furukawa M., Inoue M., Saiki K. and Yamada K. 1998, "The role of tip leakage vortex breakdown in compressor rotor aerodynamics," ASME Paper No.98-GT-239
9) Hofman W. and Ballmann J. 2002, "Tip clearance vortex development and shock-vortex-interaction in a transonic axial compressor rotor," AIAA Paper No. 2002-0083
10) Wilke I. and Kau H.-P., 2002, "A numerical investigation of the influence of casing treatments on the tip leakage flow in a HPC front stage," ASME GT-2003-38481, 2003.